JOURNAL OF SOLID STATE CHEMISTRY 113, 312–319 (1994)

On the Polymorphism in Lanthanum Polysulfide (LaS_2)

B. Le Rolland,* P. Molinié,† P. Colombet,* and P. F. McMillan‡,[1]

*Département Recherche et Développement—Matériaux Nouveaux, Technodes S. A., Groupe Les Ciments Français-Italcimenti, 78931 Guerville Cédex, France; †Institute des Matéreaux, CNRS-Université de Nantes, 2 rue de la Hossinière, 44072 Nantes Cedex 03, France; and ‡Materials Research Group, Department of Chemistry and Biochemistry, Arizona State University, Tempe, Arizona 85287-1604, USA

Received July 6, 1993; in revised form April 11, 1994; accepted April 13, 1994

The polymorphism in lantanum polysulfide (LaS_2) was investigated using X-ray diffraction and vibrational spectrocopy. Samples were prepared by traditional solid state techniques and by a method based on high pressure CS_2 treatment, and then subjected to various heating and cooling schedules. In agreement with previous work, monoclinic (α) and orthorhombic (β) forms were found, and a new tetragonal polymorph (γ) with the anti-Fe_2As structure was obtained in some synthesis runs. Unlike previous findings, no reversible transition bertween the α and β phases was observed. The tetragonal γ phase is most likely a spatially averaged disordered structure, with local symmetry lower then tetragonal. The CS_2 synthesis method gave rise to a disordered version of the monoclinic α phase, with broadened diffraction peaks. This material was slightly paramagnetic at room temperature and showed evidence for antiferromagnetic ordering below 50 K, unlike the ordered α and β phases, which were diamagnetic at all temperatures. Low-temperature EPR and Raman spectroscopy indicates that the behavior of the disordered α-LaS_2 is due to the presence of paramagnetic S^- defects and rapid S–S bond switching in the S–S basal planes. © 1994 Academic Press, Inc.

INTRODUCTION

The rare earth polysulphides, with general formula LnS_2, are currently thought to crystallize in a variety of phases based on the anti-Fe_2As structure, based primarily on studies using X-ray powder diffraction (1–13). Many of these compounds have been reported to have some degree of sulfur deficiency, although careful structural and thermodynamic studies indicate that at least some of the "nonstoichiometric" materials correspond to a mixture of phases (14–16). In particular, the orthorhombic β form of LaS_2 (9) appears to be a stoichiometric compound (14, 16). This is in contrast to the selenide, which forms a well-characterized compound $LaSe_{1.9}$ in addition to stoichiometric $LaSe_2$ (17).

"Ideal" LnS_2 with the anti-Fe_2As structure would be tetragonal (space group D_{4h}^7: $P4/nmm$), with $a_0 \approx 4$ Å and $c_0 \approx 8$ Å (taking c normal to the planes of S atoms), with two formula units per primitive cell (Fig. 1). All LnS_2 polymorphs observed to date are distorted from this ideal structure, by the formation of S–S pairs within the planes of S atoms normal to c (11, 18–20). This distortion, along with the possibility of doubling along the c axis (9, 12), gives rise to a series of potential superstructures of the anti-Fe_2As structure. For the light rare earths (Ln = La, Nd). LnS_2 unit cells have been reported as "pseudocubic" ($\sim 2a_0$, $\sim 2a_0$, $\sim c_0$), tetragonal ($\sim 2a_0$, $\sim 2c_0$), orthorhombic ($\sim 2a_0$, $\sim a_0$, $\sim 2c_0$), or monoclinic ($\sim 2a_0$, $\sim a_0$, $\sim c_0$; $\beta \sim 90°$) (1–13).

Dugué *et al.* (9) obtained an orthorhombic phase of LaS_2 (Z = 8), now termed the β-LaS_2 phase (12), by reaction of La_2S_3 + S at 750°C, and single crystals were grown using a KI–KCl flux. The crystal structure of this material was refined within space group $Pnma$ (9). Several different choices of crystallographic axes have been used in previous structural studies of LnS_2 phases. In the present work, we always choose the c axis to be oriented normal to the basal planes of S atoms for all LnS_2 superstructures, to remain consistent with the conventional choice of unique axis for the underlying anti-Fe_2As structure (Fig. 1). With this choice of c axis, the setting for the orthorhombic β-LaS_2 phase studied by Dugué *et al.* becomes $Pnam$, with a = 8.131(5), b = 4.142(2), and c = 16.34(1). (In fact, based on comparison of infrared and Raman spectroscopic data (21), it is likely that this phase is noncentrosymmetric, with space group $Pna2_1$). Bénazeth *et al.* (12) obtained a monoclinic form (α-LaS_2), with cell parameters a = 8.13 Å, b = 4.03 Å, c = 8.18 Å, α = 90° within space group $P2_1/b$ (with the unique (2_1) axis in the basal plane parallel to the a axis: $P2_1/b$ 1 1 with cell choice 1). These workers observed that mixtures of the α and β phases were obtained in synthesis runs at temperatures near 750°C and proposed (a) that the α and β phases represented respectively low- and high-temperature forms of LaS_2, and (b) that the two were related by a reversible phase transition near 750°C. In the

[1] To whom correspondence should be addressed.

0022-4596/94 $6.00
Copyright © 1994 by Academic Press, Inc.
All rights of reproduction in any form reserved.

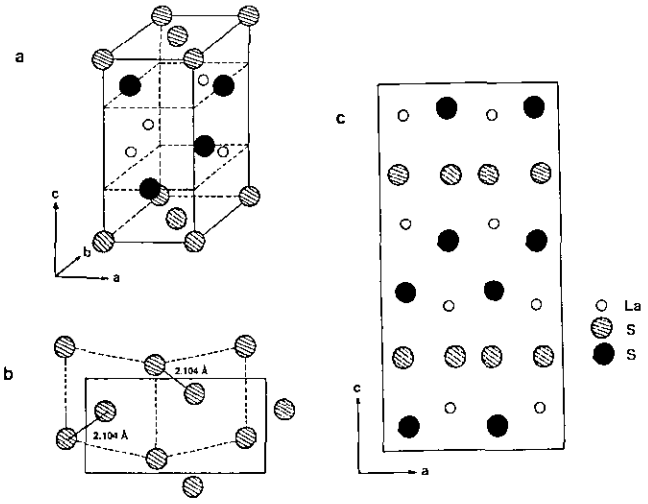

FIG. 1. (a) The idealized anti-Fe_2As structure of LaS_2. The larger and smaller circles correspond to sulfur and lanthanum, respectively. (b) The structural distortion accompanying S–S bond formation in the {001} plane, to formally give $(S_2)^{2-}$ anion groups (S–S bond distances correspond to those for the β-LaS_2 phase (9)). (c) Structure of the orthorhombic (β) polymorph of LaS_2 projected on the a–c plane, showing the doubled c axis compared with the parent anti-Fe_2As cell (9, 12).

present study, we have reinvestigated the relationship between the α and β forms of LaS_2 (Table 1). In addition, we describe a further, disordered (γ) form of LaS_2 with an averaged tetragonal anti-Fe_2As structure, which appears as a product in some annealing experiments of the α phase (Table 1, Fig. 1).

TABLE 1
Representative Synthesis and Annealing Conditions for LaS_3 Polymorphs

Starting material	Heating schedule	Product(s)
LaS_2 (α')	820°C, 168 hr, slow cooling (20°C/hr)	$\gamma^a + \alpha'$
LaS_2 (α')	840°C, 336 hr, quench into ice water	γ
LaS_2 (α')	840°C, 337 hr, slow cooling (20°C/hr)	$\gamma^a + \alpha'$
LaS_2 (α')	750°C, 168 hr, slow Cooling (20°C/hr)	β
LaS_2 (α')	840°C, 327 hr, slow cooling (20°C/hr)	$\beta^a + La_2S_3$
LaS_2 (α')	900°C, 168 hr, quench into ice water	$La_2S_3{}^a + \beta$
La_2S_3 + S	710°C, 192 hr, quench into ice water	$\alpha^a + \beta$
La_2S_3 + S	750°C, 504 hr, slow cooling (20°C/hr)	β
La_2S_3 + S	820°C, 192 hr, slow cooling (20°C/hr)	α
La_2S_3 + S	830°C, 264 hr, quench into ice water	$\alpha^a + \beta^b$

[a] Denotes majority phase.
[b] Trace identified by Raman spectroscopy.

TABLE 2
Unit Cell Parameters for LaS_2 Polymorphs

Polymaorph	Preparation	Space group	Cell parameters (Å)
α LaS_2	La_2S_3 + S; 192 hr; 820°C	$P2_1/b$ 1 1	a = 8.1740(5) α = 90.0° b = 4.1258(2) c = 8.1824(5)
α' La S_2	CS_2 method; 500°C	$P2_1/b$ 1 1	a = 8.179(2) α = 90.0° b = 4.122(1) c = 8.187(1)
β LaS_2	La_2S_3 + S; 504 hr; 750°C	*Pnam* or $Pna2_1$	a = 8.145(1) b = 4.138(1) c = 16.364(2)
γ LaS_2	Heat α' LaS_2; 168 hr; 800°C	*P4/nmm*	a = 4.0782(2) c = 8.1587(6)
γ LaS_2	La + 3S; 850–950°C; 7 days	*P4/nmm*	a = 4.147 c = 8.176

We have recently developed a new technique for synthesis of lower metal sulfides, involving treatment of the oxides or hydroxides under high (0.1–15 MPa) CS_2 pressure at low temperatures (350–600°C) (22, 23). This technique allows easy synthesis of higher transition metal and rare earth polysulfide compounds with minimal sulfur deficiency and has been used to prepare the polysulfides of La, Ce, Pr, and Nd (21). The LaS_2 phase prepared by this method from La_2O_3 at 500°C could be indexed within a monoclinic unit cell, with cell parameters close to those reported by Bénazeth *et al.* (12) for α-LaS_2 (Fig. 1, Table 2). In contrast to the powder diffraction pattern of α-LaS_2 synthesized by conventional methods, many of the peaks for the monoclinic phase obtained by the CS_2 method are broad and unresolved (Fig. 1), indicating structural disorder. To simplify the present discussion, we refer to the monoclinc phase obtained by low-temperature, high CS_2 pressure treatment as α'-LaS_2.

EXPERIMENTAL

The samples of α'-LaS_2 were synthesized via the high pressure CS_2 method (21), from La_2O_3 or $La(OH)_3$ at 500°C for 4 days (22, 23). These were then subjected to various heat treatments to investigate the relations between the different phases of LaS_2 (Table 1). In addition, some samples were synthesized directly from La_2S_3 and elemental sulfur, at temperatures between 710 and 830°C (9, 12) (Table 1). All samples were characterized by X-ray powder diffraction, using an Inel diffractometer with a solid state position sensitive multichannel detector and Cu$K_{\alpha 1}$ radiation (Fig. 2). Cell parameters were obtained by least-squares refinement (Table 2). The different phases were also distinguished by infrared and Raman spectroscopy (Figs. 3, 4). Unpolarized Raman spectra were obtained with a Dilor Microdil 28 multichannel instrument, using the 514.5-nm line of an argon ion laser for sample excitation. Powder infrared spectra were obtained

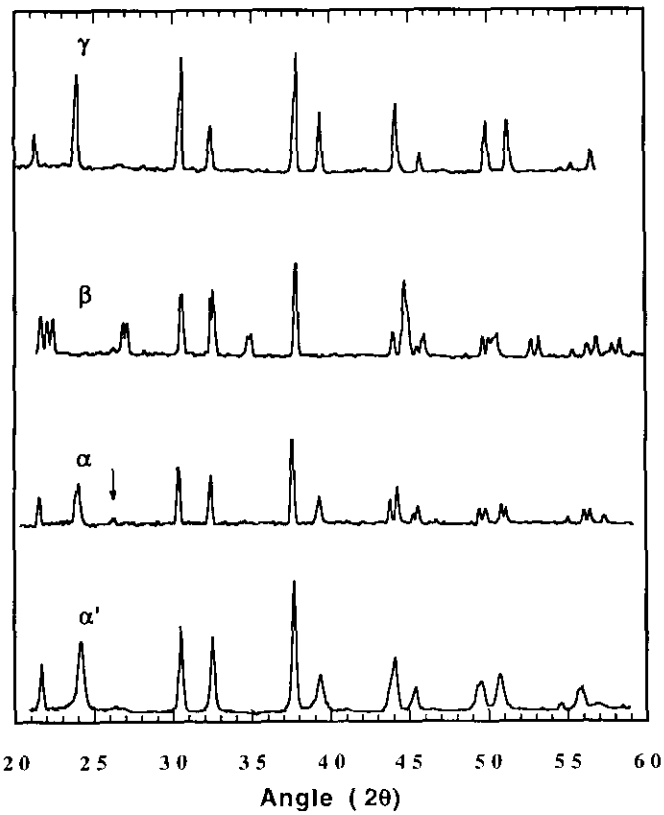

FIG. 2. Powder X-ray diffraction patterns for the α, α', β, and γ polymorphs of LaS_2. The arrow on the α LaS_2 pattern indicates the 111 reflection, indicating the doubling of the a axis relative to the parent anti-Fe_2As cell.

between 50 and 600 cm^{-1} with a Nicolet SX 20C interferometer. Samples were mixed with vaseline and mounted on a polyethylene plate.

Magnetic susceptibilities were measured from 5–300 K on 50–150 mg samples using a Quantum Design SQUID magnetometer. ESR measurements were performed with an IBM-Bruker ER-200D spectrometer at 9.4 GHz. The first derivative of the absorption was monitored by modulating the magnetic field at 100 kHz. Electrical resistivities were measured on pressed powders via the four-point probe method, using Cu wire contacts and a Keithley 616 electrometer.

RESULTS AND DISCUSSION

Crystallography and Vibrational Spectroscopy

The unit cell of the monoclinic α-LaS_2 phase is doubled along the a direction compared with the parent anti-Fe_2As structure, due to formation of S–S pairs (Fig. 1). This doubling is indicated by a weak reflection at $2\theta = 25.45°$, due to the 111 reflection of a $P2_1/b$ lattice with $a = 8.1740$ Å, $b = 4.1258$ Å, $c = 8.1824$ Å, $\alpha = 90.00°$ (Fig. 2, Table

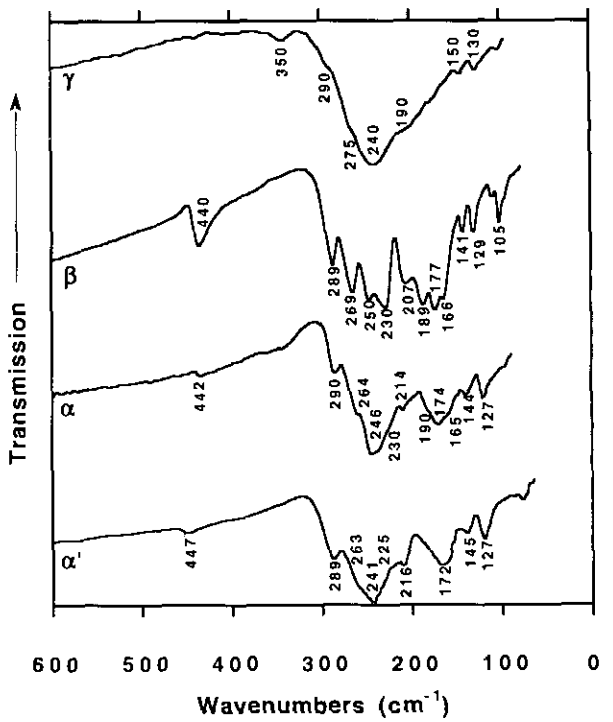

FIG. 3. Powder infrared absorption spectra for the α, α', β, and γ polymorphs of LaS_2.

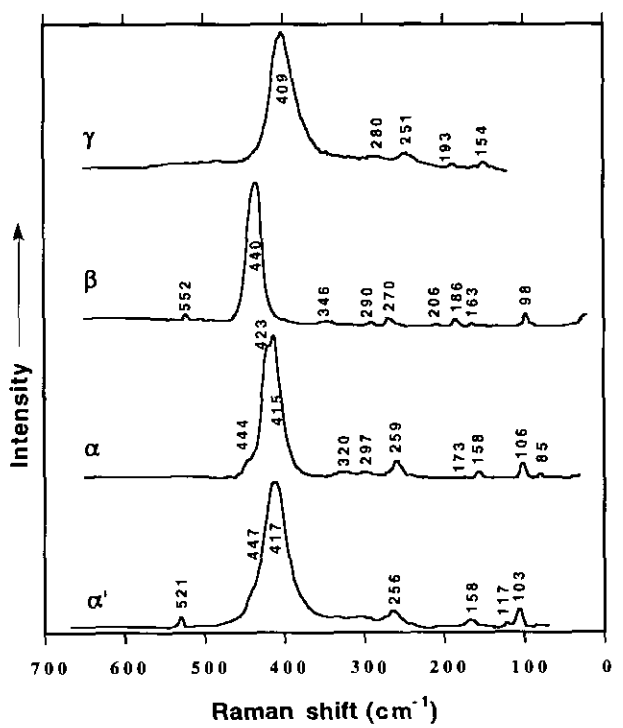

FIG. 4. Unpolarized Raman spectra of the α, α', β, and γ polymorphs of LaS_2 (a higher resolution spectrum of the α polymorph in the region of the S–S stretching vibration (near 420 cm^{-1}), which clearly shows the two peaks at 415 and 423 cm^{-1}, is shown in Fig. 6).

2). The structure is isotypic with the stoichiometric form of $LaSe_2$ (24), with all of the atoms in general positions. The powder diffraction pattern of α'-LaS_2, prepared via the high pressure CS_2 method, is compared with that of α-LaS_2 in Fig. 2. The two patterns are almost identical, but the peaks of α'-LaS_2 are broader and several sets of lines are unresolved, indicating some degree of structural disorder in this material.

The infrared and Raman spectra of the α and α' phases of LaS_2 are presented in Figs. 3 and 4. From symmetry analysis, the expected vibrational modes for α-LaS_2 are

$$\Gamma_{vib} = 9\ Ag\ (R) + 9\ Bg\ (R) + 8\ A_u\ (IR) + 7\ B_u\ (IR),$$

where R and IR indicate Raman and infrared activities, respectively. The powder infrared spectrum of α'-LaS_2 shows obvious peaks at 442, 290, 246, 214, 174, 144, and 127 cm^{-1}, with shoulders near 264, 230, 190, and 165 cm^{-1}, nearly identical to that of α-LaS_2 (Fig. 3). (The broad peak near 620 cm^{-1} observed by Le Rolland *et al.* (21) for α'-LaS_2 and CeS_2 was not reproduced in this study and was most likely due a trace of impurity phase. In addition, the list of peak frequencies given for α'-LaS_2 (21) included several weak features which were due to noise in the spectrum.) The Raman spectrum of α-LaS_2 shows strong peaks at 425 and 417 cm^{-1} and weaker features at 444, 320, 297, 259, 173, 158, 106, and 85 cm^{-1} (Fig. 4). The intensity of the 444-cm^{-1} shoulder showed some variation between different samples and could be due in part to a trace of β-LaS_2 present along with the α-LaS_2 phase. The Raman spectrum previously obtained by Golovin *et al.* (25) is for an approximately equal mixture of the two phases. The spectra of the α- and α'-phases are similar, except that the 425 and 417 cm^{-1} peaks are not resolved for α'-LaS_2, and some of the weaker features appear with different relative intensities (Fig. 4).

The cell parameters for the orthorhombic β form of LaS_2 (9) obtained in the present study (using the noncentrosymmetric choice of space group (21) in setting $Pna2_1$, with the c axis normal to the S atom planes) are $a = 8.145_1$, $b = 4.138_1$, $c = 16.364_2$. The crystallographic relationship between the α and β phases involves doubling the c axis motif of La^{3+} . . . S^{2-} stacking (12) (Fig. 1). The infrared and Raman spectra of β-LaS_2 are shown in Figs. 3 and 4 for comparison with the other phases of LaS_2. From symmetry analysis, the expected vibrational modes for β-LaS_2 are

$$\Gamma_{vib} = 17\,A_1\,(R, IR) + 18\,A_2\,(R) + 17\,B_1\,(R, IR) + 17\,B_2\,(R, IR).$$

As expected, a large number of peaks are observed in the Raman and IR spectra, with multiple coincidences (21).

During some annealing experiments on $\alpha'$$LaS_2$, prepared via the high pressure CS_2 method (Table 1), a further phase was identified by X-ray diffraction (Table 2, Fig. 2). The X-ray pattern of this material is similar to that of the disordered α' phase, but the lines are sharper, and there is no clear indication of the 111 peak at 26.45° (although some preparations indicated very weak intensity in this region). This pattern could be indexed successfully within the tetragonal space group $P4/nmm$ of the anti-Fe_2As structure, with $a_0 = 4.0872_2$ and $c_0 = 8.1587_6$. This could correspond to the tetragonal $LaS_{1.91}$ reported by Eliseev *et al.* (8), but the γ-LaS_2 phase prepared in this study is most likely stoichiometric, as discussed below. The infrared and Raman spectra of this phase are quite different to those of the α and β polymorphs (Figs. 3 and 4). The infrared spectrum shows a single strong band at 235 cm^{-1} with shoulders near 290, 275, and 190 cm^{-1} and weak features at 350, 150, and 130 cm^{-1} (Fig. 3). The Raman spectrum shows a single broad, asymmetric band at 409 cm^{-1} and weak features at 280, 251, 193, and 154 cm^{-1} (Fig. 4). These spectra can be interpreted in a first-order manner by considering only the overall structure. The fact that there is substantially less structure in the infrared absorption spectrum than for the α and β polymorphs is consistent with the presence of a higher symmetry structure with a smaller crystallographic unit cell, and the lack of obvious infrared and Raman coincidences implies the presence of a center of inversion, as expected for the anti-Fe_2As structure. However, closer examination of the spectra indicates that this anti-Fe_2As modification of LaS_2 is not fully ordered, but corresponds to a spatially averaged, disordered structure. The principal infrared and Raman bands are much broader than those for the α- and β-LaS_2 polymorphs. This type of band broadening is generally indicative of structural disorder. In addition, the expected infrared and Raman bands for an ideal anti-Fe_2As structure are

$$\Gamma_{vib} = 2A_{1g}\,(R) + B_{2g}\,(R) + E_g\,(R) + 2A_{2u}\,(IR) + 2E_u\,(IR).$$

The precise number of distinct bands in the infrared and Raman spectra is difficult to evaluate, but there is certainly a greater number than predicted from the symmetry analysis for the ideal structure. This indicates that the local symmetry is lower than $P4/nmm$, and it is likely that the structure of our γ-LaS_2 consists of local domains of, for example α-LaS_2, arranged in a disordered fashion.

The Relationship between the α and β Structures

The structures of the rare earth polysulfides LnS_2 are derived from the anti-Fe_2As structure and consist of double sheets of $(LnS)_n$ stoichiometry which alternate with planes of sulfur atoms (Fig. 1). The unit cell dimensions

of this idealized anti-Fe_2As structure are approximately 4 × 4 × 8 Å. In the real LnS_2 structures, adjacent S atoms in the sulfur planes are displaced toward each other to form ordered pairs, giving the nominal formula $Ln_2^{3+}(S_2)^{2-}(S^{2-})_2$ (5, 13–15) (Fig. 1). The simplest ordering pattern would involve formation of an S–S bond between the same pair of atoms in each unit cell, to give a phase with a monoclinic or triclinic 4 × 4 × 8 Å cell. This structure has not yet been observed for any LnS_2 polymorph. The 8 × 4 × 8 Å structure found in α- and β-LaS_2 (12) is shown in Fig. 1. This has a doubled *a* axis repeat due to inversion of the S–S bond formation pattern in adjacent cells of the underlying anti-Fe_2As structure. The β-LaS_2 phase described by Dugué *et al.* (9) is also doubled in the *c* direction, resulting from a half-unit-cell translation of the $(LaS)_n$ layers (12) (Fig. 1).

In our synthesis studies, the CS_2 method always yielded the α′ form of LaS_2, with broadened X-ray peaks. The degree of structural order appeared to vary between synthesis runs, based on the degree of resolution and relative intensities of peaks in the X-ray powder diffraction pattern. Different annealing experiments on this material gave several different results (Table 1). One run of 7 days at 750°C resulted in complete transformation to the orthorhombic (8 × 4 × 16 Å cell) β phase. Two further runs at 840 and 900°C for 14 and 7 days, respectively, also yielded the β phase, accompanied by La_2S_3. In both of these runs, elemental S was observed to have condensed at one end of the reaction tube. In contrast, three runs at 820–840°C for 7–14 days gave the disordered, spatially averaged anti-Fe_2As (γ) phase described above, along with untransformed α′ in two cases (Table 1).

Some samples of LaS_2 were also synthesized directly from La_2S_3 + S, for comparison with the results of Bénazeth *et al.* (12). In one synthesis at 750°C (8 days), β-LaS_2 was obtained in pure form. Following Dugué *et al.* (9), large crystals (approximately 100–300 mm) were obtained by heating this material in a KI–KCl bath at 750°C for 21 days. Bénazeth *et al.* (12) concluded that LaS_2 underwent a reversible, but quenchable, transition between the α and β phases at 750°C. We carried out one synthesis of LaS_2 from La_2S_3 + S at 820°C (8 days), followed by a slow descent in temperature (20°C/hr). This resulted in a sample of pure monoclinic α-LaS_2 (Table 1). A second run at the same temperature (11 days), followed by a rapid quench in ice water also gave almost pure α-LaS_2, accompanied by a trace of β phase. The X-ray pattern showed only peaks for the α phase, but the presence of β-LaS_2 was indicated by Raman spectroscopy. We also carried out a further LaS_2 synthesis run at 710°C (8 days), followed by a rapid quench, and again obtained a mixture of α and β phases, this time obvious by powder X-ray diffraction (Table 1).

From the ensemble of synthesis and annealing runs, we cannot accept the conclusions of Bénazeth *et al.* (12), that rapidly quenching LaS_2 from above 750°C results in recovery of β-LaS_2, and that the transition between the α and β polymorphs of LaS_2 is reversible above and below 750°C. The findings of Ref. (12) are also not in accord with the fact that large single crystals of β-LaS_2 can be obtained at 750°C, following an initial synthesis at 700°C (9).

Because of their structural similarity, it is likely that the free energies of the α and β polymorphs of LaS_2 are quite similar. Because of the ease in growing single crystals of β-LaS_2 compared with the α phase, and because β-LaS_2 seems to be the most common product of long-term annealing experiments (taking into account the ensemble of our data for the LaS_2 (CS_2) and La_2S_3 + S experiments), we propose that β-LaS_2 is likely to be the thermodynamically stable form, at least for temperatures above 700°C. The fact that α′-LaS_2 is consistently obtained in synthesis experiments using the high pressure CS_2 method at temperatures near 500°C could suggest that the α polymorph is the more stable at low temperature. This is in general agreement with part of the conclusions of Bénazeth *et al.* (12), although the synthesis products at lower temperature may well be influenced by kinetic factors. We were unable to carry out the β–α transformation at any temperature.

Because diffusion in sulfides is slow, reaction temperatures on the order of at least 700°C are generally required for solid state syntheses. This is also likely to be the case for the reconstructive transformation between the α and β polymorphs of LaS_2, which requires interdiffusion of La and S atoms, or reorganization of the relative arrangement of the $(LaS)_n$ and S atom planes (12). However, above approximately 700°C, the vapor pressure curve of sulfur begins to increase steeply (14), and high-temperature annealing experiments are complicated by loss of S from the material. If there is a sufficient temperature gradient within the reaction tube, S can condense on the cooler parts of the tube and be removed from the sample. This is especially important if the reaction tube is long relative to the hot region of the furnace. In addition, the quench rate can play a role in determining whether S vapor can recombine with the sample during cooling. It is obvious that a combination of these factors can result in considerable variability in the reaction products obtained, as noted by Bénazeth *et al.* (12), depending on details of the preparation method.

Compositions of LnS_x Phases

As noted in the Introduction, several previous studies have indicated that some phases of LnS_2 compounds in general, and lanthanum polysulfides in particular, are sulfur deficient, with quoted compositions ranging from

$LaS_{1.75}$ to LaS_2. Vasil'eva *et al.* (14) measured the sulfur vapor pressure above heated single crystals of β-LaS_2 (with an analyzed starting composition of $LaS_{2.02\pm0.02}$) and observed only a smooth vapor pressure curve, with no breaks in slope which might indicate the formation of sulfur-deficient phases (a break in slope was observed at high temperature due to the α–β transformation of La_2S_3). The nonstoichiometric phases reported by previous authors could be due to a mix of LaS_2 and La_2S_3 in their reaction products, consistent with the results of our annealing experiments. In the cases where sulfur was observed to condense on the cold end of the reaction tube in our studies, La_2S_3 was found in the reaction products along with β-LaS_2. In the 750°C annealing experiment, the α' phase transformed completely into the stoichiometric β phase (Table 1), conforming the LaS_2 stoichiometry of the starting material. This reasoning also holds for the disordered γ phase (Table 1). Eliseev *et al.* (3) have described a tetragonal anti-Fe_2As structure for neodymium polysulfide, with lattice parameters similar to those refined here for γ-LaS_2, which they concluded was sulfur deficient. However, in that study, the composition of $NdS_{1.95}$ was deduced on the basis of calculated R factors for assumed sulfur contents of 2.00, 1.95, and 1.80. This determination could be affected by the presence of structural disorder, which we have shown to be important for the tetragonal γ-LaS_2 phase prepared in our study.

The Disordered Anti-Fe2As Structure

The tetragonal γ-LaS_2 structure could only be prepared by annealing from the α' structure, never from the orthorhombic β phase in any of our studies. This observation could indicate that the γ phase represents a disordered intermediate during the reconstructive phase transformation between the metastable α' phase and the stable β polymorph. Evidence that the γ phase does not represent a true anti-Fe_2As structure, but a spatially averaged disordered phase, was presented above on the basis of the infrared and Raman spectra. In addition, conductivity measurements carried out on pressed powders show that γ-LaS_2 is insulating, unlike $LaTe_2$ with a true anti-Fe_2As structure, which is an electronic conductor (26). A further sample of the tetragonal phase, with lattice parameters slightly different from that obtained by annealing α'-LaS_2 (Table 2), was obtained by heating elemental La and S in a 1 : 3 ratio at 850–950°C for 7 days. This structural variability is consistent with different degrees of structural order. It is interesting to note that the c dimension of γ-LaS_2 prepared from the α' phase is slightly shortened relative to its parent material. This could indicate some buckling of the basal sulfur planes at the α–β transformation proceeds. This would be consistent with the low frequency of the principal S–S stretching vibration, observed in the Raman spectrum, relative to the α, α', and β phases (Fig. 4).

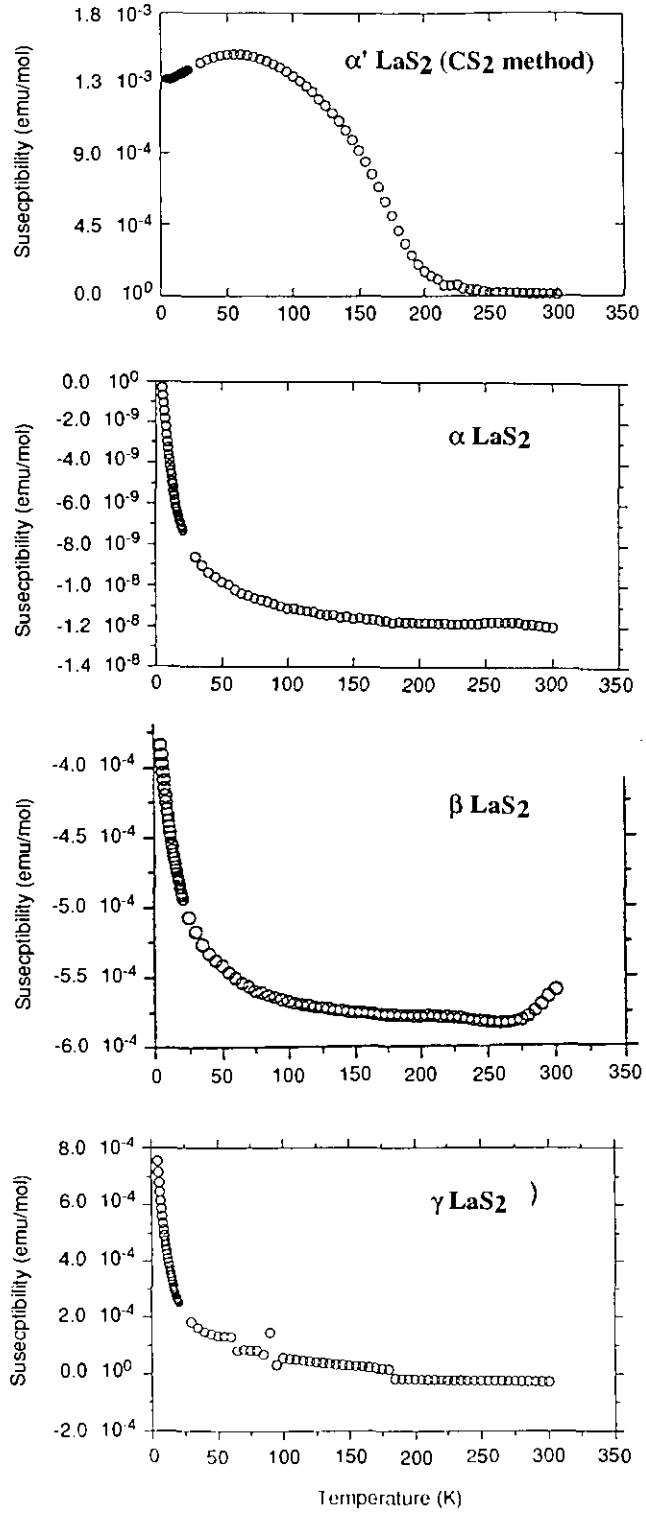

FIG. 5. Magnetic susceptibilities of the α, α', β, and γ polymorphs of LaS_2.

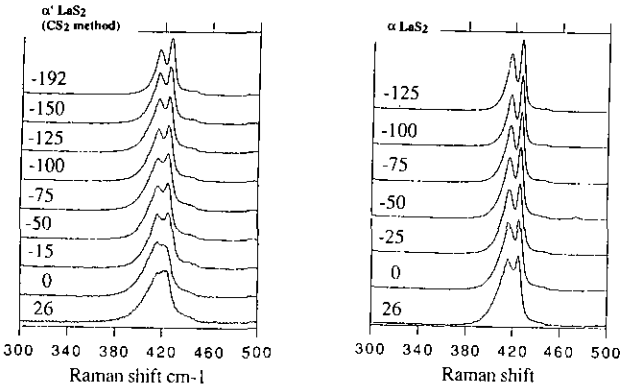

FIG. 6. Low-temperature Raman spectra of the α and α' polymorphs of LaS_2 in the region of the S–S stretching vibration. Temperatures are given in °C.

Further Characterization of the α'-Phase

In order to more fully characterize the α-LaS_2 prepared in our low temperatures CS_2 synthesis experiments and better understand the origin of the broadening in the X-ray diffraction peaks, we measured the magnetic susceptibility of all the LaS_2 phases, and carried out a Raman spectroscopic study of α- and α'-LaS_2 at low temperature.

The results obtained by SQUID magnetometry are shown in Fig. 5. The α- and β-LaS_2 phases prepared by conventional solid state synthesis are diamagnetic at room temperature, as expected from the crystal structure, and show a Curie tail below 50 K due to localized paramagnetic impurities. In contrast, the α' phase is slightly paramagnetic at room temperature and exhibits a characteristic $\chi(T)$ curve for an antiferromagnetic substance at low temperature, with T_N near 50 K.

The low-temperature Raman spectra for this phase are shown in Fig. 6. At room temperature, the S–S stretching region contains a single broad band at 420 cm^{-1}. Starting at −15°C, this band begins to be resolved into two components, and by −192°C there are two peaks near 415 and 422 cm^{-1}, identical to the spectrum of α-LaS_2 at the same temperature (Fig. 6). This behavior is reversed on warming the sample. This observation suggests that the α'-LaS_2 form is related to α'-LaS_2 by a displacive structural transition with a low activation energy barrier. We can relate this to the observed paramagnetic behavior by the following structural model. We presume that the low-temperature CS_2 synthesis results in formation of an α-LaS_2 structure containing a significant proportion of "wrong" S–S bonds (Fig. 7). If the structure is nearly stoichiometric, these must result in the presence of paramagnetic S centers. However, all that is required to for such S^- defects to bond with their neighbor to form a S–S bond is for the S atoms to undergo a vibrational displacement in the S–S plane, resulting in translation of the S^- defect (Fig. 7). At room temperature, this itinerant paramagnetism will result in the observed paramagnetic susceptibility, and the S–S stretching vibration is smeared out. As the temperature is lowered, the rate of S–S bond interchange is slowed down, and the paramagnetic S^- defects become localized. The structure probed on a vibrational time scale contains regions of α-LaS_2, resulting in the observed low-temperature Raman spectrum, and the magnetic defects begin to order, in an antiferromagnetic manner.

We have measured the ESR spectrum of α'-LaS2 from 190 to 110 K. Consistent with the proposed structural model, a single sharp resonance with $g = 2$ is observed at high temperature, corresponding to an itinerant electron signal. Below 170 K, this is joined by a broad signal at slightly lower field, which would correspond to the localized paramagnetic center (Fig. 8a). The measured resistivity of α'-LaS_2 also shows a slight discontinuity near 180 K (Fig. 8b), which can be associated with the freezing of the polaron conductivity mechanism.

CONCLUSIONS

From our synthesis and annealing experiments, we conclude that the α and β forms of LaS_2 probably do correspond respectively to low and high-temperature polymorphs, although the α phase may be only kinetically stabilized in lower temperature synthesis runs, and they are not related by a reversible phase transition under normal experimental conditions. A γ form of LaS_2 with an X-ray diffraction pattern corresponding to the ideal anti-Fe_2As structure is found in some synthesis experiments, but its vibrational spectra confirm this phase to represent a spatially averaged disordered material. Fi-

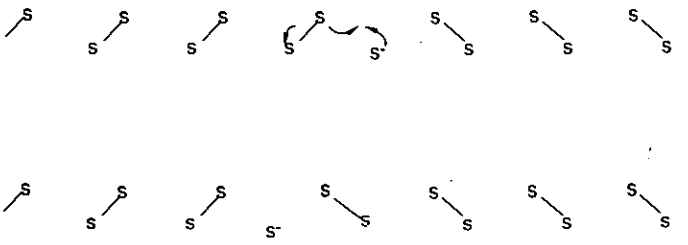

FIG. 7. Proposed model to rationalize the observed magnetic behavior and Raman spectra of α'-LaS_2. The CS_2 synthesis at low temperatures results in formation of "wrong" bonds within the α-LaS_2 structure, giving rise to paramagnetic S^- defects. These defects move within the lattice via S–S bond interchange, which occurs on a vibrational time scale at room temperature. Each S–S pair corresponds to a diamagnetic $(S_2)^{2-}$ unit, as required by charge balance within the structure. The arrows in the top part of the figure indicate movement of a single electron to (a) form a new S–S bond and (b) create a new S^- defect, translated one lattice unit to the left (bottom drawing). As the sample is cooled, this S–S bond interchange is slowed down, and the paramagnetic centers become localized, giving rise to the antiferromagnetic order.

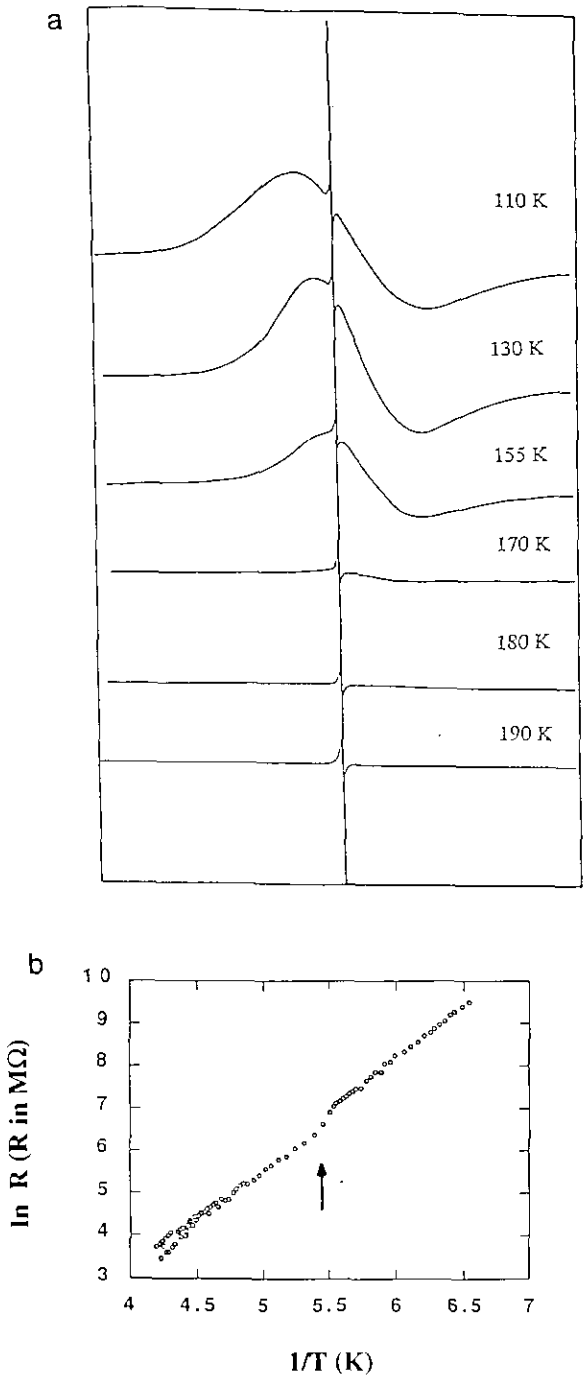

FIG. 8. (a) Low-temperature ESR spectra of powdered α'-LaS_2 sample. The field increases left to right. (b) Electrical resistivity of a pressed powder sample of α'-LaS_2, showing the slight discontinuity near 180 K.

nally, an α' form of LaS_2 prepared by CS_2 treatment of oxides and hydroxides at low temperatures has broadened X-ray lines. This material shows interesting antiferromagnetic behavior at low temperature, and its Raman spectrum indicates a displacive transition to the α form. The ensemble of magnetic susceptibility, Raman, ESR, and conductivity data suggests that this transition is associated with the presence of paramagnetic S^- defects in the synthesized material, accompanied by rapid S–S bond interchange reactions. These bond-making and -breaking reactions slow down at lowered temperatures, resulting in localization of the paramagnetic defects and onset of the magnetic ordering behavior.

ACKNOWLEDGMENT

This work was partly supported by Materials Research Group grant DMR-9121570.

REFERENCES

1. J. Flahaut, M. Guittard, and M. Patrie, *Bull. Soc. Chim. Fr.* **26,** 1917 (1959).
2. S. A. Ring and M. Tecotzky, *Inorg. Chem.* **3,** 182 (1964).
3. A. A. Eliseev, S. I. Uspenskaya, and A. A. Fedorov, *Russ. J. Inorg. Chem.* **16,** 786 (1971).
4. A. A. Eliseev, S. I. Uspenskaya, and T. A. Kalganova, *Russ. J. Inorg. Chem.* **17,** 1222 (1972).
5. S. I. Uspenskaya and A. A. Elisee, *Russ. J. Inorg. Chem.* **17,** 1344 (1972).
6. Y. Yanagisawa and S. Kume, *Mater. Res. Bull.* **8,** 1241 (1973).
7. E. M. Loginova, A. A. Grizik, N. M. Ponomarev, and A. A. Eliseev, *Izv. Akad. Nauk SSSR Neorg. Mater.* **11,** 749 (1975).
8. A. A. Eliseev, V. A. Tolstova, and G. M. Kuz'micheva, *Russ. J. Inorg. Chem.* **23,** 1759 (1978).
9. J. Dugué, D. Carre, and M. Guittard, *Acta Crystallogr. Sect. B* **34,** 403 (1978).
10. Y. Yanagisawa, F. Kanamura, and S. Kume, *Acta Crystallogr, Sect. B* **35,** 137 (1979).
11. J. Flahaut, *in* "Handbook on the Physics and Chemistry of Rare Earths" (K. A. Gschneider, Jr., and L. Eyring, Eds.), Vol. 2, p. 1, North-Holland, Amsterdam, 1979.
12. S. Bénazeth, M. Guittard, and J. Flahaut, *J. Solid State Chem.* **37,** 44 (1981).
13. Y. Yanagisawa and S. Kume, *Mater. Res. Bull.* **21,** 379 (1986).
14. I. G. Vasil'eva, A. N. Kanev, V. G. Kamburg, and E. D. Popova, *Izv. Akad. Nauk SSSR Neorg. Mater.* **15,** 1330 (1979).
15. I. G. Vasil'eva and L. G. Gorbanova, *Izv. Sib. Otd. Akad. Nauk SSSR Ser. Khim. Nauk* **5,** 77 (1986).
16. A. B. Tagaev, V. N. Naumov, I. G. Vasil'eva, and I. E. Paukov, *Russ. J. Inorg. Chem.* **63,** 1247 (1989).
17. M. Grupe and W. Urland, *J. Less-Common Metals* **170,** 271 (1991).
18. F. Jellinek, *in* "Inorganic Sulphur Chemistry" (G. Nickless, Ed.), p. 669, Elsevier, Amsterdam/New York, 1968.
19. A. F. Wells, "Structural Inorganic Chemistry," 5th ed., Clarendon Press, London/New York, 1984.
20. F. Hulliger, *in* "Structure and Bonding in Crystals" (M. O. Keeffe and A. Navrotsky, Eds.), Vol. 2, p. 297, Academic Press, New York, 1981.
21. B. Le Rolland, P. McMillan, and P. Colombet, *C.R. Acad. Sci. Paris Sér. II* **312,** 217 (1991).
22. P. Colombet, P. Moline, and M. Spiesser, "Procédé d'élaboration de composés binaries de soufre," European patent 440516, 1991.
23. B. Le Rolland, "Les Sulfures de Terres Rares: Synthèse, Caractérisation et Valorisation," Thèse de Doctorat, Université de nantes, 1992.
24. S. Benazeth, D. Carre, and P. Laruelle, *Acta Crystallogr. Ser. B* **38,** 33 (1982).
25. Y. M. Golovin, K. I. Petrov, E. M. Loginova, A. A. Grizok, and N. M. Ponomarev, *Russ. J. Inorg. Chem.* **20,** 155 (1975).
26. T. H. Ramsey, H. Steinfink, and E. J. Weiss, *J. Appl. Phys.* **36,** 548 (1965).